TECTONICS, VOL. 17, NO. 3, PAGES, 360-378 JUNE 1998

Uplift and erosion of the San Bernardino Mountains associated with transpression along the San Andreas fault, California, as constrained by radiogenic helium thermochronometry

James A. Spotila, Kenneth A. Farley, and Kerry Sieh

Division of Geological and Planetary Sciences, California Institute of Technology, Pasadena

Abstract. Apatite helium thermochronometry provides new constraints on the tectonic history of a recently uplifted crystalline mass adjacent to the San Andreas fault. By documenting aspects of the low-temperature (40°-100°C) thermal history of the tectonic blocks of the San Bernardino Mountains in southern California, we have placed new constraints on the magnitude and timing of uplift. Old helium ages (64-21 Ma) from the large Big Bear plateau predate the recent uplift of the range and show that only several kilometers of exhumation has taken place since the Late Cretaceous period. These ages imply that the surface of the plateau may have been exposed in the late Miocene and was uplifted only ~1 km above the Mojave Desert in the last few Myr by thrusting on the north and south. A similar range in helium ages (56-14 Ma) from the higher San Gorgonio block to the south suggests that its crest was once contiguous with that of the Big Bear block and that its greater elevation represents a localized uplift that the Big Bear plateau did not experience. The structure of the San Gorgonio block appears to be a gentle antiform, based on the geometry of helium isochrons and geologic constraints. Young ages (0.7-1.6 Ma) from crustal slices within the San Andreas fault zone indicate uplift of a greater magnitude than blocks to the north. These smaller blocks probably experienced ≥3-4 km of uplift at rates ≥1.5 mm/yr in the past few Myr and would stand ≥2.5 km higher than the Big Bear plateau if erosion had not occurred. The greater uplift of tectonic blocks adjacent to and within the San Andreas fault zone is more likely the result of oblique displacement along high-angle faults than motion along the thrust fault that bounds the north side of the range. We speculate that this uplift is the result of convergence and slip partitioning associated with local geometric complexities along this strike-slip system. Transpression thus appears to have been accommodated by both vertical displacement within the San Andreas fault zone and thrusting on adjacent structures.

Paper number 98TC00378.
0278-7407/98/98TC-00378$12.00

1. Introduction

The San Bernardino Mountains (SBMs) have risen during the past few Myr in association with transpression along the San Andreas fault zone in southern California [cf. *Dibblee*, 1975; *Sadler*, 1982a; *Meisling and Weldon*, 1989]. The complex evolution of this convergent stretch of the San Andreas system and the relationship between transpression and orogeny along it are not fully understood [*Matti and Morton*, 1993; *Weldon et al.*, 1993; *Dibblee*, 1982]. At first glance, the SBMs appear to be a single structural entity because of their discrete geographic form (Plate 1). However, the range actually consists of several distinct, fault-bounded blocks that diminish in size and become more structurally complex toward the San Andreas fault zone that bounds them on the south (Figure 1). Although the uplift of the largest of these blocks has been explained by motion along the low-angle thrust fault that bounds the range on the north [cf. *Dibblee*, 1975; *Meisling*, 1984], it is unknown whether the blocks to the south were raised by the same mechanism. This is because the magnitude, form, and chronology of uplift are less well constrained in the southern part of the range.

The poor understanding of the uplift kinematics of the southern SBMs exemplifies the more general problem of determining the role that strike-slip faults play in accommodating transpression through uplift. Because it bounds the range on the south, it is possible that significant vertical motion has taken place along the high-angle faults of the San Andreas system, perhaps in concert with uplift along the thrust fault that bounds the range on the north. Alternatively, it is conceivable that the topography of the southern SBMs formed adjacent to and in conjunction with the uplift of the San Gabriel Mountains, which now lie 50 km to the northwest. Strike-slip offset of these ranges along a purely strike-slip San Andreas fault system may thus have occurred subsequent to uplift along the thrusts that bound each mountain block. These hypotheses represent very different concepts for the kinematics of the San Andreas fault. A better understanding of the timing and evolution of uplift of the range would facilitate our understanding of transpression along the San Andreas fault and is important for assessing the degree of current activity on all of the bounding structures.

To learn more about the evolution of uplift and how it has accommodated transpression in the SBMs, the history and magnitude of uplift of the major blocks must be

constrained. Existing data on the timing of bedrock uplift from strata adjacent to the range do not allow us to discriminate different histories for different blocks. There are also no recognized structural or stratigraphic datums that constrain the degree of exhumation and rock uplift [cf. *England and Molnar*, 1990] of the southern blocks relative to the north [*Dibblee*, 1975]. To better understand these aspects of the uplift history, we utilized the recently developed low-temperature thermochronometer of radiogenic helium ([U-Th]/He) in apatite on granitic samples from the range [*Zeitler et al.*, 1987; *Lippolt et al.*, 1994; *Wolf et al.*, 1996a, 1997]. We compare these results to geologic and geomorphic observations and present new structural interpretations for the uplift of the major tectonic blocks. Thus we provide new constraints on the evolution of transpression over the last few Myr and on the role the San Andreas fault has played during uplift of elements of the SBMs.

2. Geological Background

The SBMs are an isolated, high range within the central Transverse Ranges province (Plate 1). They are distinct from neighboring lowlands and are separated from adjacent mountain blocks by the San Andreas and Pinto Mountain faults (Figure 1). The northern two thirds of the range consists of the broad plateau of the Big Bear (BB) block, which is characterized by gentle highland topography surrounded by steep northern and southern escarpments and moderately sloping eastern and western flanks (Plate 1 and Figure 1). The steep northern and southern escarpments of the plateau are bound by the North Frontal thrust system and Santa Ana thrust, respectively. To the south, the range is narrower and significantly higher and consists of rugged, east-west trending ridges and intervening canyons. This topography is similar to the basic form predicted for continental plateaus, in which high peaks form along windward margins due to isostatic compensation of deep incision [*Masek et al.*, 1994; *Molnar and England*, 1990]. The high, elongate ridges of the SBMs are separated by major faults within intermontane valleys, however, suggesting the SBMs consist of a series of distinct tectonic blocks.

The San Gorgonio (SG) block is the largest of these southern fault-bounded tectonic blocks and has steep northern and southern margins, moderate eastern and western flanks, and a rugged crest that includes the highest peak in southern California (San Gorgonio Peak, 3506 m). This block is separated from the low Santa Ana Valley on the north by unnamed high-angle faults [*Sadler*, 1993] and is bound on the south by the Mill Creek strand of the San Andreas fault zone, across which lie the smaller Wilson Creek (WC) and Yucaipa Ridge (YR) blocks (Figure 1). These are not as high as the SG block but are slightly steeper (Plate 1). To the south of these lie the Mission Creek and San Bernardino strands of the San Andreas fault zone, across which sits the rugged Morongo block. The southern third of the SBMs thus consists of higher and steeper topography, which could indicate more rapid erosion due to more recent or greater tectonic or isostatic uplift than the BB block may have experienced.

Uplift of the modern SBMs initiated sometime after the Miocene epoch. Pre-Pliocene strata, particularly in the northwestern part of the range, do not record evidence of the SBMs as a major topographic high (Figure 1) [cf. *Meisling and Weldon*, 1989; *Weldon*, 1986; *Meisling*, 1984; *Sadler*, 1993; *Sadler et al.*, 1993; *Allen*, 1957; *Woodburne*, 1975]. Late Miocene basalt flows in several isolated places atop the BB block also suggest that uplift is younger than ~6-10 Myr ago, because they were probably associated with crustal extension prior to the most recent transpression [*Neville and Chambers*, 1982]. Further stratigraphic evidence shows uplift of the range began between 2 and 3 Myr ago. These data include facies and provenance changes in clastic deposits of the Old Woman sandstone on the north, the Phelan Peak Formation on the northwest, and the San Timoteo Formation on the south [*May and Repenning*, 1982; *Meisling and Weldon*, 1989; *Reynolds and Reeder*, 1986]. Excepting the northwesternmost part of the range, however, the stratigraphic record lacks the resolution to constrain the uplift history of the SBMs subsequent to its initiation. Thus it is not known whether the mountain rose en masse or the different blocks rose independently and whether the uplift proceeded at uniform rates or had more complicated histories. Geodetic evidence argues that the entire region has uplifted substantially in most recent time [*Castle and Gilmore*, 1992].

In several localities in the SBMs and Mojave Desert, basalts and Miocene sediments overlie a horizon of deeply weathered granite that may have begun forming during the more humid climate of the late Miocene [*Oberlander*, 1972]. Both the covered and the uncovered weathered granite surfaces are nearly contiguous across the BB block and extend over large regions of gentle topography separated by incised stream canyons (Plate 1 and Figure 1). This suggests that the basic form of the plateau and its deep weathering predate uplift [*Dibblee*, 1975; *Sadler and Reeder*, 1983; *Meisling*, 1984]. The extensive distribution of this surface could further suggest there has been limited erosion of the BB block subsequent to initiation of uplift. If so, then its gross shape may reflect the uplift of the portions of the range that it covers [*Dibblee*, 1975]. The vertical displacement of the plateau relative to the surrounding lowlands may thus be loosely constrained by its topography. The entire length of the plateau (east to west) is confined by the North Frontal thrust system that dips beneath it (Figure 1), indicating that the thrust was at least partly responsible for the uplift of the BB block [*Meisling*, 1984]. The Santa Ana thrust also dips beneath the plateau and bounds part of its length on the south (Figure 1), suggesting it may have also contributed to recent uplift of the BB block [*Sadler*, 1993]. These opposing thrusts may steepen and converge into a high-angle transpressive zone at depth [*Sadler*, 1982b], or the North Frontal thrust may flatten into a decollement that undercuts the Santa Ana thrust and continues to the south [*Corbett*, 1984; *Webb and Kanamori*, 1985; *Meisling and Weldon*, 1989; *Li et al.*, 1992; *Seeber and Armbruster*, 1995].

The SG block has minor patches of weathered granite that are similar to those atop the BB block, but these are

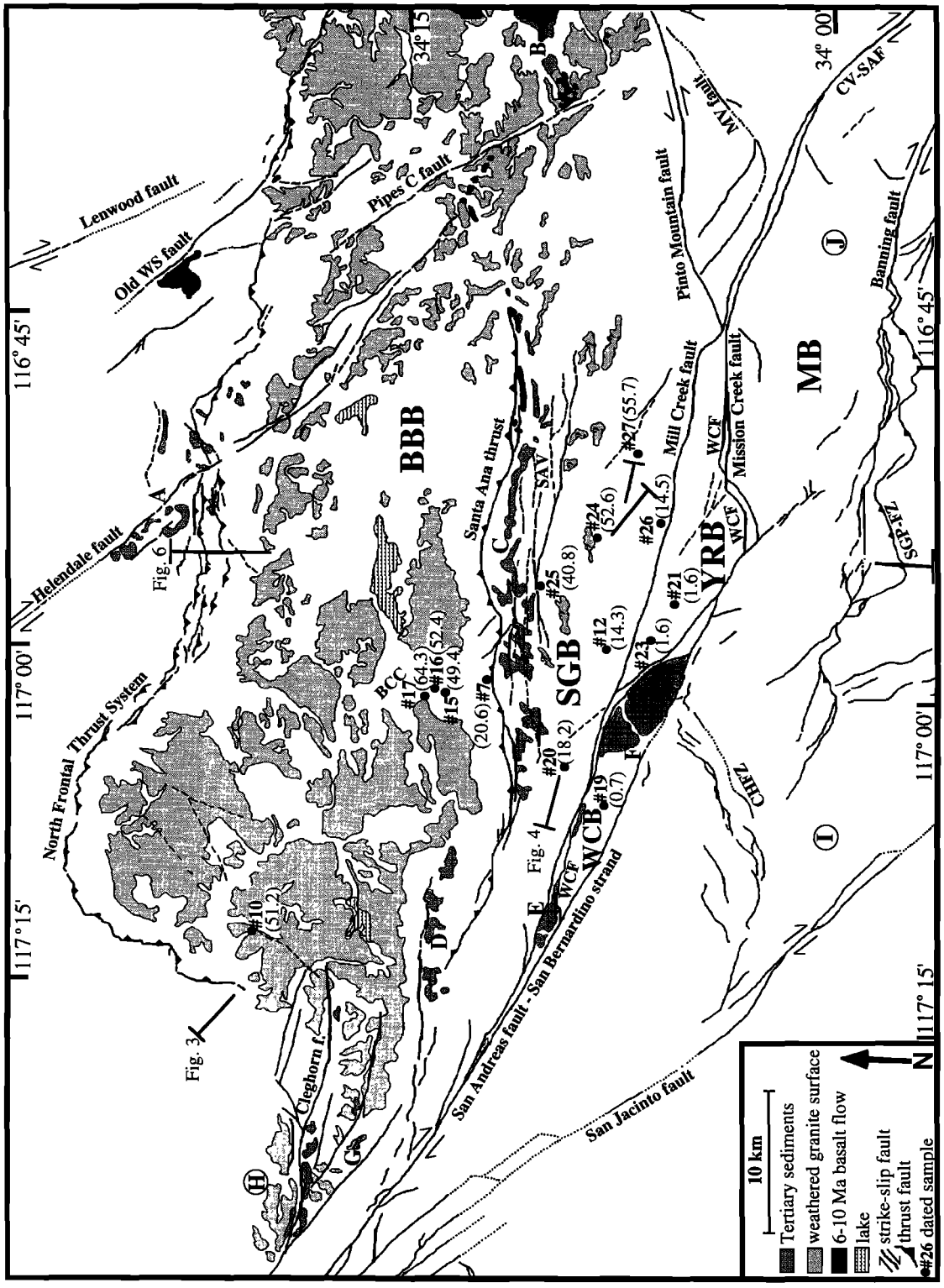
Lenwood fault
Old WS fault
Pipes C fault
MV fault
CV-SAF
Pinto Mountain fault
Banning fault
Helendale fault
North Frontal Thrust System
Santa Ana thrust
Mill Creek fault
WCF
Mission Creek fault
SGP-FZ
CHZ
San Andreas fault - San Bernardino strand
San Jacinto fault
Cleghorn f.
BCF
SAV
BBB
SGB
WCB
YRB
MB
Fig. 3
Fig. 4
Fig. 6
#10 (51.2)
#15 (20.6)
#16 (52.4)
#17 (64.3)
#7
#20 (18.2)
#19 (0.7)
#25 (40.8)
#12 (14.3)
#23 (1.6)
#24 (52.6)
#27 (55.7)
#26 (14.5)
#21 (1.6)
34°15
34° 00'
116° 45'
117° 00'
117° 15'
N
10 km
Tertiary sediments
weathered granite surface
6-10 Ma basalt flow
lake
strike-slip fault
thrust fault
#26 dated sample

Figure 1.

not directly correlative because of the intervening low Santa Ana Valley and the faults therein (Figure 1). The preservation of the Mio-Pliocene Santa Ana sandstone in the valley shows that it is a structural low rather than an erosional canyon. The sandstone overlies deeply weathered granite in the valley as well, but this cannot be uniquely correlated with that atop either the BB or SG blocks because of intervening faults. Thus the relative vertical displacement between the blocks is uncertain [*Dibblee*, 1975; *Sadler and Reeder*, 1983]. The crest of the SG block is about 1 km higher than the southern crest of the BB block, despite the fact that the intervening Santa Ana thrust has moved the BB block upward relative to the SG block [*Sadler*, 1993] (Plate 1 and Figure 1). The lack of correlative, deeply weathered surfaces atop the YR, WC, and Morongo blocks, within the San Andreas fault zone, and the likelihood of large lateral offsets along the San Andreas obscure the relative vertical motion between these blocks and the SG and BB blocks. The lack of such relict surfaces atop these southern blocks is also consistent with the more rugged topography that suggests greater erosion than on the SG and BB blocks.

Because the magnitude of uplift is not constrained for the southern blocks, the degree to which they have been uplifted by a southward continuation of the North Frontal thrust system or the more proximal high-angle strands of the San Andreas fault zone is unknown. In the northwesternmost part of the range, where the stratigraphic record is more detailed, it has been argued that the San Andreas fault produced the substantial uplift and tilting of the western San Bernardino arch [*Meisling and Weldon*, 1989]. Lack of suitable marker horizons and datable, syntectonic strata in the southern SBMs have thus far obscured similar study of the role the San Andreas fault has played in uplift there.

3. Methods

We have attempted to document the low-temperature cooling history of the SBMs to constrain the history and magnitude of rock uplift and exhumation associated with the construction of the modern range. Given that the SBMs consist of several tectonic blocks defined on the basis of geomorphology and the distribution of major faults, we compared the cooling histories of each to learn about their relative surface uplift and exhumation. In each block, we collected multiple samples of granitic rock that maximized relief and minimized lateral separations in order to document the age-elevation relationship through a near-vertical crustal section.

Thermochronometry of radiogenic helium in apatite ($Ca_5[PO_4]_3[F, Cl, OH]$) is a recently developed method that constrains the low-temperature cooling history of rocks [*Zeitler et al.*, 1987; *Lippolt et al.*, 1994; *Wolf et al.*, 1996a, 1997; *House et al.*, 1997]. This method is based on the thermally activated diffusion and retention of ^4He, which is produced by the radioactive decay of uranium and thorium series nuclides. A "helium age" is calculated from the measured quantities of the parent and daughter isotopes and represents the amount of time required to radiogenically produce a given amount of ^4He assuming no initial helium and secular equilibrium in the decay series. Because helium is nearly completely lost by diffusion from apatite over geological timescales at temperatures >100°C and is only partially retained (because of slow, partial diffusion) at temperatures of 40°-100°C, this method is sensitive to the cooling rocks experience as they rise through the "helium partial retention zone" of the uppermost crust (a few kilometers depth for typical geothermal gradients). This technique is sensitive to lower temperatures than other

Figure 1. Tectonic and simplified geologic map of the San Bernardino Mountains (location shown on Plate 1), showing sample locations and average ages (in Myr), as in Table 1. The major tectonic blocks, Quaternary faults [adapted from *Matti and Morton*, 1993], Tertiary sediments, Miocene basalts (6-10 Ma [*Neville and Chambers*, 1982]), and the preuplift, weathered granitic surface [*Oberlander*, 1972] are also indicated. The distributions of the weathered surface, faults of the North Frontal thrust system, and the faults between the Santa Ana thrust and the San Gorgonio block are based on airphoto mapping and field investigations by the first author. Letters refer to Tertiary deposits [from *Dibblee*, 1964, 1968; *Bortugno and Spittler*, 1986] as follows: A, Old Woman sandstone (2-3 Ma, records initiation of uplift [*May and Repenning*, 1982]); B, eastern Santa Ana sandstone [*Sadler*, 1993]; C, Santa Ana sandstone (4-15 Ma, preuplift facies and source [*Sadler*, 1993]); D, Crowder Formation [*Sadler*, 1993]; E, Potato sandstone (~13 Ma, preuplift strike-slip basin [*Sadler et al.*, 1993]); F, Mill Creek Formation (10-13 Ma, preuplift strike-slip basin [*Sadler et al.*, 1993]); G, Crowder Formation deposited atop the weathered surface [*Meisling and Weldon*, 1989]; H, general location of the San Francisquito, Vaqueros, and Cajon Formations (Paleocene to Miocene, preuplift), Crowder Formation (17-9.5 Ma, preuplift facies and source), and Phelan Peak Formation (4-1.5 Ma, facies and source record uplift) [*Woodburne*, 1975; *Meisling and Weldon*, 1989]; I, general location of Mount Eden Formation (Pliocene) and San Timoteo Formation (Plio-Pleistocene, syntectonic) [*Reynolds and Reeder*, 1986]; and J, general location of Coachella Fanglomerate (Miocene), Imperial Formation (Mio-Pliocene, marine), Painted Hill Formation (Pliocene, nonmarine), and Cabezon Fanglomerate (Pleistocene, synuplift) [*Allen*, 1957; *Proctor*, 1968]. Straight lines show locations of elevation profiles in Figures 3, 4, and 5. Abbreviations are as follows: BBB, Big Bear block; BCC, Bear Creek Canyon; CHFZ, Crafton Hills fault zone; CV-SAF, Coachella Valley-San Andreas fault; MB, Morongo block; MV fault, Morongo Valley fault; Old WS fault, Old Woman Springs fault; Pipes C fault, Pipes Canyon fault; SAV, Santa Ana Valley; SGB, San Gorgonio block; SGP-FZ, San Gorgonio Pass fault zone; WCB, Wilson Creek block; WCF, Wilson Creek fault; and YRB, Yucaipa Ridge block.

thermochronometers. For example, with a constant cooling rate of 10°C/Ma, the helium closure temperature [*Dodson*, 1973] is 75°C, significantly lower than for apatite fission track annealing (~105°C) [*Wolf et al.*, 1996a].

Helium ages are thus useful for learning about recent exhumation, even though they are a function of cooling history and do not necessarily represent ages of specific geologic events or cooling through a specific temperature. A single helium age does not uniquely determine the time-temperature path of a rock, but suites of helium ages can significantly narrow the range of plausible thermal histories, particularly when combined with other geologic and thermochronometric data. In addition, isochronous surfaces constructed from helium ages can serve as marker horizons that constrain postcooling deformation or relative vertical displacements, which is particularly useful in crystalline rocks [*Wolf et al.*, 1997]. This is true only when exhumation during cooling was laterally uniform and isotherms in the upper crust were approximately horizontal. Techniques for interpreting apatite helium ages are presented in detail elsewhere [*Wolf*, 1997; *Wolf et al.*, 1997; *House et al.*, 1997].

We have dated replicate aliquots of apatite from granitic rocks in the SBMs. Samples of apatite consisted of ~10-20 crystals (~0.1-0.3 mg) of roughly 0.1- to 0.4-mm dimension. Apatites were selected on the basis of morphology, size, and the absence of visible defects. Crystals were also carefully screened for U- and Th-bearing silicate inclusions, which can produce anomalously old helium ages [*House et al.*, 1997]. Two of the samples analyzed in this study (15 and 16) had high concentrations of zircon inclusions and were difficult to date accurately. Helium was outgassed in a high-vacuum furnace and measured by quadrupole mass spectrometry in the Noble Gas Laboratory of the California Institute of Technology following the procedures of *Wolf* [1997]. Analytical precision of helium measurements (typically ~0.1-1.0 pmol ^{4}He) is estimated to be ~3-4% (1σ), based on reproducibility of standards [*Wolf*, 1997]. Helium contents of samples were corrected for alpha ejection, a phenomenon in which helium that is produced near a crystal surface is expelled because of the long stopping distance of alpha particles during radioactive decay (independent of cooling history or diffusion). Following the procedures of *Farley et al.* [1996], we corrected for this using a coefficient (F_T, typically 0.65-0.85) derived from the average size and shape of individual crystals in each sample. We estimate the uncertainty of measuring F_T to be ~2-3% (1σ), based on repeated measurements on single samples. Following helium outgassing, samples were retrieved from the furnace, dissolved in HNO_3, and their U and Th contents were measured by isotope dilution with an inductively coupled plasma mass spectrometer (ICP-MS) at the California Institute of Technology with ~2% analytical precision. The 1σ uncertainties of these different measurements (He, F_T, U, and Th) propagate to yield an uncertainty of about ±5% (1σ) for individual helium ages. Because we replicated analyses, our precision on average helium ages should be about ±7% (2σ). This is consistent with our observed external reproducibility of helium ages (2σ = 8% for samples with >0.1-pmol helium). We conservatively use 8% (2σ) errors in this study.

4. Results

We have measured replicate helium ages on 14 samples of Mesozoic granitoid rocks whose crystallization ages range from the ~90-Myr-old Cactus quartz monzonite, which makes up the majority of the SBMs basement [*Dibblee*, 1982], to a 215-Myr-old megaporphyritic monzogranite [*Frizzel et al.*, 1986]. The samples span elevations ranging between 652 m and 3506 m within the principal structural blocks of the range (Figure 1). Four samples from the steep southern flank of the BB block and two samples from the YR block comprise nearly vertical series, whereas other samples are spread laterally over the BB block, SG block, and YR and WC blocks. Our measured helium ages and related data are listed in Table 1 and are plotted against elevation in Figure 2.

Helium ages from the five samples in the BB block are early Miocene and older. The highest sample (17, 2113 m) is from atop the weathered plateau and gave the oldest age of 64.3 ± 5.1 Ma. A second sample (10, 1329 m) from atop the plateau about 20 km to the northwest gave a similar average age of 51.2 ± 4.1 Ma, suggesting isochronous surfaces tilt very slightly to the northwest (Figure 3). The helium ages beneath sample 17 (samples 15, 16, and 7) from the steep transect along the side of Bear Creek Canyon decrease roughly linearly with elevation to 20.6 ± 1.6 Ma (sample 7, 1233 m). Together these make a very steep age-elevation gradient of ~50 ± 8 Myr/km. If the isochrons between these samples are slightly tilted as they are to the northwest, the elevation difference that defines this gradient may be slightly different than the paleodepth difference (i.e., during cooling) between samples. In addition, the gradient defined by the upper three samples (17, 15, and 16) alone is lower (~30 Myr/km) (Figure 2), showing that the young age of sample 7 affects the gradient strongly. Given that this sample was located only several hundred meters from the Santa Ana thrust (Figure 1), it may be anomalously young as a consequence of hot fluids circulating near the fault zone. There is no way of determining whether this is the case, however, and thus we interpret the measured ages at face value.

Six helium ages from the SG block are older than middle Miocene, comparable to the old ages from the BB block. As in the BB block, the cooling history recorded by these ages predates the recent uplift of the SBMs. Helium ages from the high ridge line of the SG block (55.7 ± 4.5 atop San Gorgonio Peak, sample 27) are very similar to the ages from the weathered plateau surface atop the BB block. The ages decrease roughly with elevation to 18.2 ± 1.5 Ma at the Santa Ana River (sample 20, 756 m). The age-elevation gradient of the SG block is best constrained by the sample pairs that have the greatest vertical separation and the smallest lateral separation, given that the samples are laterally spaced over more than 20 km distance. Two such sample pairs (27 and 26, 24 and 26)

Table 1. Helium Ages and Associated Data

Sample	Longitude x Latitude	Elev., m	Rock Type	He, pmol	Th, ppm	U, ppm	Mass, mg	F_T	Corrected Age, Ma	Average Age*, Ma
				Big Bear Block						
7(1)	117.0073x34.1872	1233	qtz. monz.	0.108	16.4	11.7	0.083	0.78	20.2	20.6±1.6
(2)				0.135	11.8	12.3	0.099	0.82	21.0	
10(1)	117.1993x34.3221	1329	qtz. monz.	0.976	10.9	9.43	0.349	0.86	51.2	51.2±4.1
(2)				0.994	10.9	8.40	0.388	0.87	51.1	
15(12)	117.0186x34.2137	1614	qtz. monz.	0.066	26.6	15.3	0.017	0.71	49.4†	49.4±3.9
16(2)	117.0161x34.2173	1812	qtz. monz.	0.496	8.12	5.69	0.269	0.87	52.8	52.4±4.2
(4)				0.279	20.3	14.4	0.065	0.81	51.9†	
17(1)	117.0235x34.2247	2113	qtz. monz.	1.213	16.8	7.09	0.360	0.87	66.5	64.3±5.1
(3)				0.449	12.0	5.26	0.201	0.85	62.0	
				San Gorgonio Block						
12(3)	116.9783x34.1162	1526	qtz. monz.	0.144	8.17	9.68	0.191	0.83	14.9	14.3±1.1
(3b)				0.147	12.1	9.70	0.176	0.86	14.9	
(4)				0.090	9.06	9.00	0.142	0.83	13.1	
20(1)	117 0703x34.1362	756	qtz. monz	0.483	20.0	17.8	0.280	0.85	17.2	18.2±1.5
(2)				0.489	21.6	18.7	0.239	0.86	19.1	
24(1)	116.8934x34.1247	3311	qtz. monz.	0.450	9.58	5.35	0.265	0.87	48.8	52.6±4.2
(2)				0.479	12.5	5.83	0.219	0.84	56.4	
25(1)	116.9290x34.1588	1861	qtz. monz.	0.777	21.8	18.1	0.166	0.83	46.3	40.8±3.3
(2)				1.162	15.7	19.4	0.307	0.86	36.1	
(3)				1.363	16.7	27.1	0.239	0.87	40.1	
26(2)	116.8894x34.0833	1899	qtz. monz.	0.376	17.0	17.8	0.258	0.86	14.7	14.5±1.2
(3)				0.151	2.61	15.6	0.150	0.83	14.3	
27(1)	116.828x34.101	3506	qtz. monz.	1.724	29.8	24.2	0.222	0.83	56.9	55.7±4.5
(3)				1.025	34.7	25.8	0.134	0.79	54.5	
				Wilson Creek Block						
19(3)	117.0955x34.1102	652	granodiorite	0.0033	27.7	16.0	0.051	0.73	0.76	0.7±0.2††
(4)				0.0084	29.5	16.4	0.160	0.78	0.55†	
				Yucaipa Ridge Block						
21(1)	116.9453x34.0078	2323	granodiorite	0.032	58.6	22.9	0.147	0.81	1.38	1.6±0.5††
(2)				0.089	48.4	23.3	0.361	0.86	1.57	
(3)				0.114	61.7	26.7	0.366	0.86	1.67†	
23(1)	116.9676x34.0897	1387	granodiorite	0.058	7.75	24.0	0.299	0.85	1.68	1.6±0.5††
(2)				0.038	6.18	15.1	0.373	0.87	1.35	
(3)				0.081	6.49	20.8	0.451	0.85	1.80†	

Numbers in parentheses are replicates from the same rock. Abbreviation elev. is elevation and qtz. monz. is quartz monzonite.

* With 2σ error equal to 8%.

† Samples on which helium was measured with greater precision on a different mass spectrometer (MAP) at Caltech.

†† The 2σ error limits on samples with small amounts of helium are ±30%, see text.

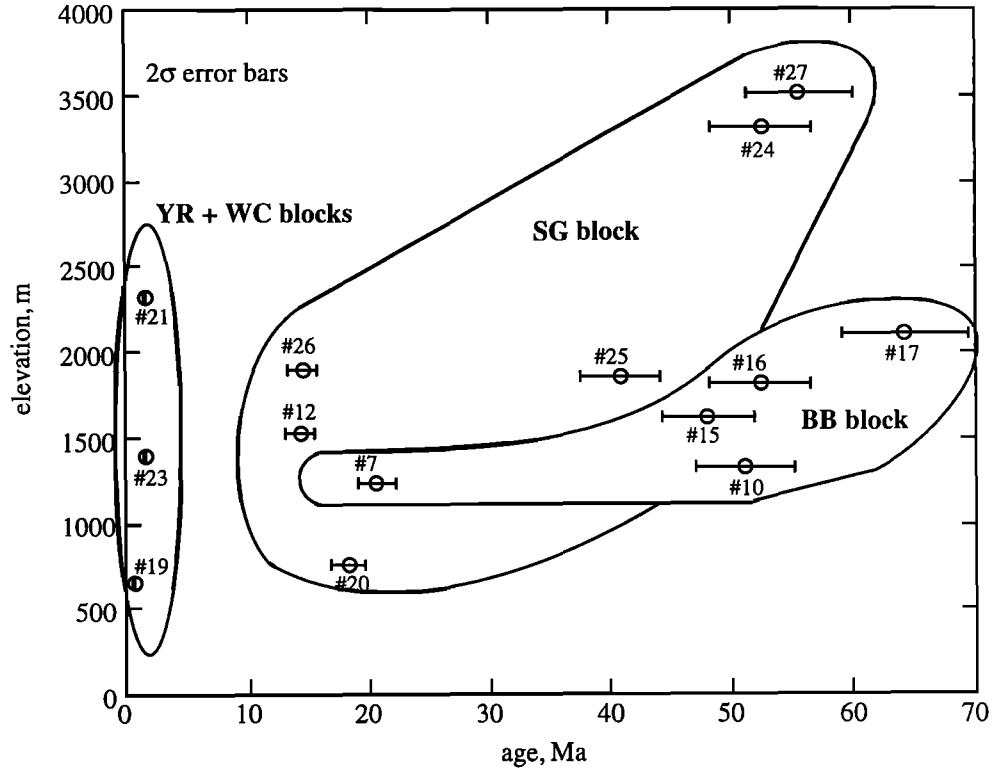

Figure 2. Elevation-age plot for individual helium ages of samples dated in this study. Numbers refer to samples in Table 1 and Figure 1. The ages are grouped within the main blocks as shown (YR+WC, Yucaipa Ridge and Wilson Creek; SG, San Gorgonio; and BB, Big Bear blocks). The tectonic blocks are defined by the location of faults and geomorphology, as discussed in text. Error bars (8%, 2σ) are shown for averaged ages, which appear as circles.

give gradients of ~26 Myr/km, roughly comparable to the BB block.

The samples from blocks within the strands of the San Andreas fault zone yielded helium ages that are far younger than those from the SG and BB blocks to the north. Two samples (21 and 23) from the YR block yielded average ages of 1.6 ± 0.5 Ma, and one sample (19) from the WC block yielded an average age of only 0.7 ± 0.2 Ma. These young ages suggest very rapid cooling that is contemporaneous with the recent construction of the SBMs. The YR block samples came from a continuous body of granodiorite [*Dibblee*, 1968] but were separated vertically by nearly 1 km (2323- to 1387-m elevation). The WC block is separated from the YR block by the Wilson Creek fault [*Matti and Morton*, 1993], and the elevation of the sample was the lowest in this study (652 m). The apatite helium contents associated with these young ages were low enough to approach the detection limit on the quadrupole mass spectrometer (0.01-0.1 pmol ^{4}He). Because line blanks were typically 10-30% of these helium measurements, the uncertainty in these young ages is much higher than for the other samples. The reproducibility of these ages averaged ~15% (Table 1), and we have thus assigned a 2σ error limit of ±30% (about ±0.5 Ma) for the young samples from the southern blocks.

5. Interpretations

5.1 Big Bear Block

The old helium ages from the BB block do not record the post-Miocene cooling history associated with recent uplift of the SBMs, but they do limit the magnitude of exhumation that could have taken place during the uplift of the modern range. The preservation of the weathered granite, basalts, and sediments atop the surface of the plateau led previous workers to suggest that postuplift erosion has been confined to incision of minor stream courses and that the shape of the plateau reflects structural relief [*Dibblee*, 1975; *Sadler and Reeder*, 1983]. The helium ages are a useful test of this suggestion, because they should reflect a lack of significant exhumation associated with uplift of the modern range.

The oldest helium age from the BB block (64.3 ± 5.1 Ma, sample 17, 2113 m) is located near granitic samples from the plateau surface that yield ~70 Ma K/Ar (biotite) ages [*Miller and Morton*, 1980]. Biotite K/Ar ages represent the time at which samples cooled through a closure temperature of about 300°C, so that cooling of more than 200°C had to have occurred over just a few Myr for granitic rocks atop the plateau. This rapid cooling episode (>50°C/Myr) may represent either a major Late

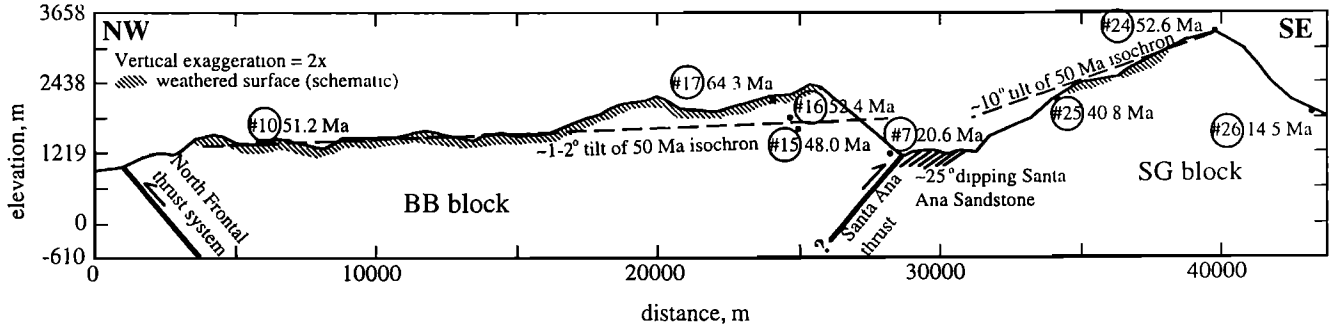

Figure 3. Elevation profile from northwest to southeast along the Big Bear and San Gorgonio blocks. The weathered surface, shown schematically by hachures, tilts more steeply northwestward than the 50-Ma helium isochron. Helium ages from Bear Creek Canyon are projected onto this section. Line of section shown in Figure 1.

Cretaceous exhumation event associated with the Laramide orogeny [cf. *George and Dokka*, 1994; *Foster et al.*, 1991] or cooling of a shallowly emplaced granitic pluton [cf. *House et al.*, 1997; *Wolf et al.*, 1997]. Following this rapid cooling, sample 17 had to have been cooler than the temperature range of helium partial retention (<40°C or <2 km depth for a typical geothermal gradient) to have achieved such an old age. This suggests that there has been very little erosion from the top of the BB block since the Late Cretaceous. It is also consistent with the idea that granitic weathering atop the plateau has been preserved because of very limited erosion since the Miocene [*Oberlander*, 1972].

The suite of younger helium ages beneath sample 17 along the side of Bear Creek Canyon (samples 16, 15, and 7) (Figures 1 and 2) further constrains the thermal history of the BB block. The steep age-elevation profile of these samples (~50 Myr/km) is indicative of very slow cooling but is not easy to interpret. Because the profile consists of only one uniform segment without a break in slope, there is no segue into the more recent thermal history of the block. The difficulty in interpreting such age profiles has been discussed in fission track studies [cf. *Gleadow and Fitzgerald*, 1987]. However, there are two end-member thermal histories involving slow cooling that are consistent with geologic constraints, which we explore below. First, the steep age-elevation gradient could have been produced by very slow, uniform uplift through the helium partial retention zone, in which case different ages would correspond to the same closure temperature, and the age gradient could be inverted for the approximate uplift rate (~0.02 mm/yr). The second possibility is that the ages represent temporary stagnation (zero uplift) in the zone, in which case the age gradient would have steepened with time (deeper samples retaining less helium than higher, cooler ones) and represent an exhumed helium partial retention zone when subsequently uplifted to the surface [*Wolf et al.*, 1997; *Wolf*, 1997].

Numerical solutions to the helium production/diffusion equation determine the helium age that would be produced for a hypothetical thermal history of a given rock (based on calibration of Durango apatite [*Wolf*, 1997; *Wolf et al.*, 1996b]). Such numerical modeling can thus be used to test the viability of these end-member thermal histories for the BB block. To be viable, a thermal history must produce the observed set of helium ages at different elevations and meet the thermal constraints of other data, which in this case include the K/Ar ages from atop the plateau and the likelihood that the plateau was exposed to deep weathering and deposition of basalt flows in the late Miocene [*Oberlander*, 1972]. Implicit assumptions to this test are that exhumation and cooling were uniform over the horizontal distance between samples and that the present-day elevation difference between samples approximates the difference in paleodepth during exhumation and cooling.

In each case, the numerical model is run with the above constraints for different geothermal gradients on hypothetical samples separated by depths corresponding to present elevation differences. In the first thermal history, slow, constant cooling/uplift follows rapid unroofing in the Late Cretaceous. For example, the helium age from the uppermost sample (64.3 ± 5.1 Ma, sample 17) could have been produced if it cooled from 300°C to 60°C between 70 and 67 Ma, then cooled slowly (<1°C/Myr) to 15°C by 10 Ma, and remained at ambient surface temperature until the present. This thermal history could have produced the observed helium ages beneath sample 17 only if the geothermal gradient was ~50°C/km throughout the Tertiary, which is geologically unlikely [*Lachenbruch et al.*, 1985]. In the second example, a prolonged period of crustal stasis follows the rapid unroofing of the Late Cretaceous, which, in turn, is followed by a short period of exhumation. For example, the helium age from the upper sample could have been produced if it cooled from 300°C to 40°C between 70 and 67 Ma, remained at 40°C until 20 Ma, and cooled to ambient surface temperature (15°C) by 10 Ma. This thermal history could have produced the helium ages of the lower samples with a more reasonable geothermal gradient of ~25°C/km. This suggests that the case of temporary crustal stasis gives a thermal history that is more consistent with helium ages for the BB block.

Although these numerical models are nonunique, the thermal history that best reproduces the available data

argues that the BB block was stable at shallow crustal depths throughout the Tertiary. Following rapid cooling in the Late Cretaceous, the uppermost sample would have sat at ~1 km depth until exhumed to the surface during the Miocene. The implied Miocene rock uplift rate of ~0.1 mm/yr would contrast with the lack of crustal motion throughout the earlier part of the Tertiary and could correlate with uplift along the Squaw Peak thrust system [*Meisling and Weldon*, 1989]. Both of the above cases show that the helium ages are consistent with *Oberlander's* [1972] proposed subaerial exposure of the top of the BB block in the late Miocene. Once exposed, the lower samples within the block (less than 1 km elevation below sample 17) would still be buried but would be cooler than the temperature range of helium partial retention, given a reasonable geothermal gradient. The subsequent uplift of the BB block along bounding thrust faults in the last few Myr [*Meisling and Weldon*, 1989; *May and Repenning*, 1982] would have displaced the surface of the plateau from the surrounding Mojave Desert, but it would have resulted in cooling that did not affect the helium ages of lower samples. The exposure of lower samples would have resulted from erosion along the margins of the block during uplift, as opposed to lowering of the entire plateau surface, and thus significant exhumation did not accompany post-3-Ma rock uplift across most of the BB block.

The geometries of isochronous surfaces in the BB block are also important. The similarity of the two helium ages from atop the plateau (samples 17 and 10, ~20 km apart) suggests that the weathered surface exposes similar structural levels on the northwest and southeast, with respect to the helium system. The weathered surface dips roughly 2°-3° northwestward from the southcentral part of the plateau [*Meisling and Weldon*, 1989], whereas the 50-Ma helium isochron dips ~1°-2° (Figure 3). While not perfectly parallel, these two horizons have roughly the same orientation, which is remarkable considering they have such different origins. The weathering may thus have developed while helium isochrons were still relatively flat, and their geometric relationship may be similar across the entire plateau. The weathered surface mimics the table-like topography of the BB block and defines an uplifted region that fits the spatial distribution of the bounding North Frontal thrust system and Santa Ana thrust (Figure 1). By analogy, the isochronous surfaces may also have a smooth shape across the plateau, indicating that they are consistent with uniform uplift of the block along the bounding thrust faults.

5.2 San Gorgonio Block

The similar range in helium ages from the SG and BB blocks suggests that the two blocks shared similar cooling histories throughout the Tertiary. Although the younger ages from the SG block (samples 20, 12, and 26) are at similar elevations as the youngest in the BB block (sample 7), the old ages (samples 27 and 24) from the top of the SG block occur more than a kilometer higher than similarly old ages in the BB block (samples 17 and 16) (Figures 2 and 3). The helium isochrons in the SG block thus span a greater range of elevation than similar isochrons in the BB block. Ages of the SG block also fail to show as simple a relationship with elevation as in the BB block (Figure 2) but have a lower age-elevation gradient. This suggests that localized uplift occurred in the SG block following the closure (cooling) of the helium system for these samples. The greater elevation span of isochronous surfaces in the SG block may thus be analogous to the greater apparent thickness of tilted sedimentary strata when not measured orthogonal to bedding.

Several lines of geologic evidence suggest that the magnitude of uplift varies systematically across the SG block and that the block was locally deformed. Patches of weathered granite along its northern crest may have once been aligned with the weathered surface atop the BB block but now sit higher and dip 10°-20° to the north [*Sadler and Reeder*, 1983] (Figure 3). The eastern and western exposures of the Santa Ana sandstone show similar orientation (10°-40° north dip [*Sadler*, 1993; *Jacobs*, 1982; *Dibblee*, 1964]), although there are faults of uncertain displacement that separate the SG block from the Santa Ana Valley (Figure 1). The very presence of the Mio-Pliocene Santa Ana sandstone in the Santa Ana Valley also argues for a gradient of increasing uplift from north to south in the vicinity of the SG block. The topography of the SG block can be described as an east-west elongate dome [*Sadler*, 1993; *Dibblee*, 1982], which is highest in the middle and tapers gently to either side. If this topography is not the result of differential erosion from east to west, then the central portion of the block has experienced the greatest uplift. This is consistent with the central exposures of the Santa Ana sandstone, which show the most intense deformation below the highest portion of the SG block [*Sadler*, 1993]. Although other geologic features, such as foliations in crystalline bedrock, do not exhibit a coherent pattern that would support or refute this structural geometry, it seems plausible that the SG block is a broad structural dome.

Helium ages should reflect a similar variation in uplift magnitude across the SG block, if the above structural interpretation is correct. If the ages are consistent with the basic structural framework presented by the geologic observations, the hypothesis that the SG block has been warped into a dome is supported.

The helium ages lack a uniform relationship with elevation, which could be the result of differential rock uplift along the 20-km-long sample transect (Figures 1 and 2). If the SG block experienced very slow cooling throughout the Tertiary in a geothermal gradient that did not vary sharply over short distances, as suggested by the similarity of ages in the BB block, then helium isochrons should have been roughly horizontal when they formed. The ages of five samples (20, 12, 24, 26, and 27) that fall roughly on an east-west axis along the SG block (Figure 1), however, form curved helium isochrons that mimic the geological evidence mentioned above (Figure 4a). Although these isochrons are only loosely defined by the data, they do show upward warping toward the center of

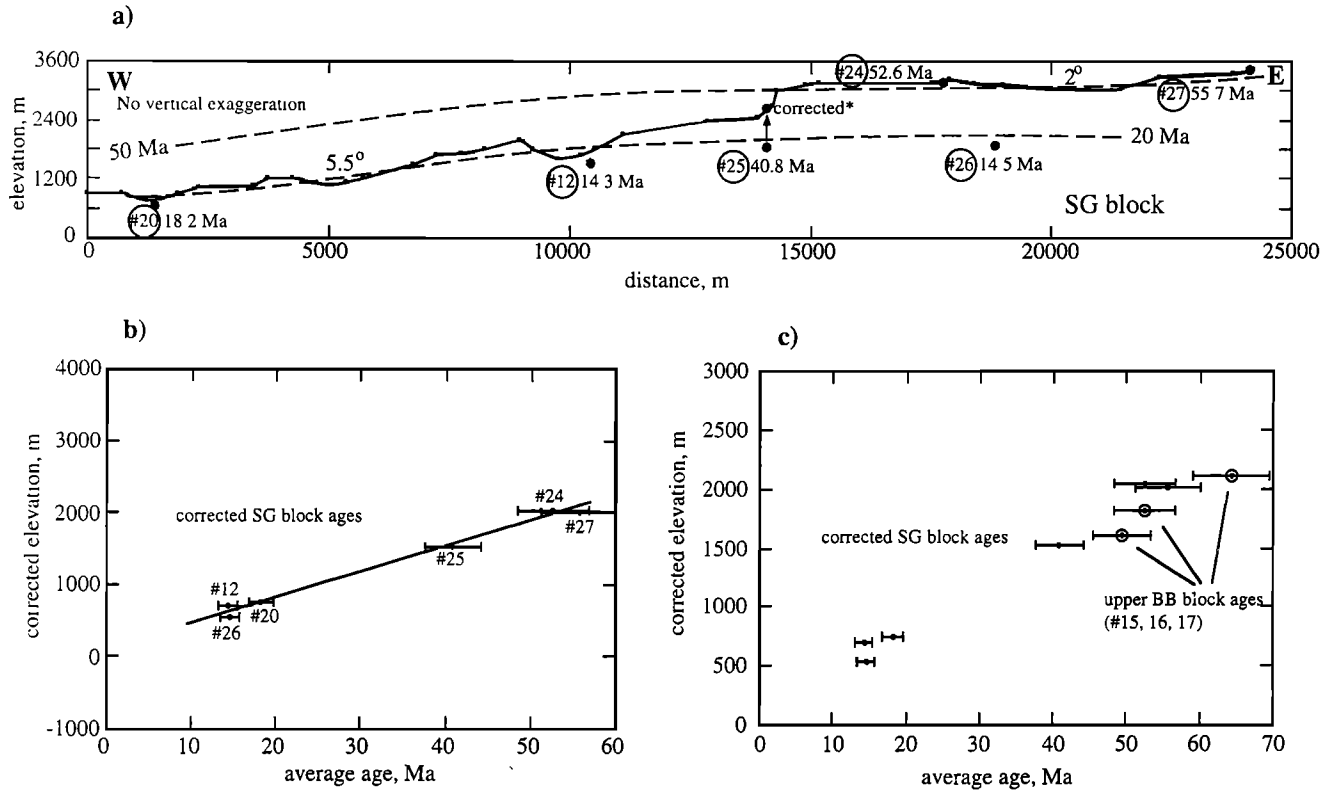

Figure 4. (a) West to east elevation profile along the ridge line of the San Gorgonio block (line of section shown in Figure 1). Profile runs from Santa Ana River on the west to San Gorgonio Peak on the east. Sample locations have been projected on to this line and are shown with their ages. Approximate isochrons (50 and 20 Ma) for helium ages are shown, both sloping 5.5° on the west and 2° in the east. Sample 25 fits these isochrons only when corrected for a 10° dip to the north, based on the slope of the patches of weathered granite. (b) Age-elevation plot of helium ages from the SG block after being corrected for the warping of the block, indicated by geologic data and the dip of isochrons shown in Figure 4a. These define a tight monotonic relationship once corrected. Samples received the following corrections: sample 12 lowered 830 m (5.5°W tilt over 8.6 km from hinge at sample 20), sample 25 lowered 1131 m (5.5°W over 11.8 km) and raised 793 m (10°N over 4.5 km from other samples), sample 24 lowered 1131 m (same as sample 25) plus 135 m (2°W over 3.9 km from sample 25), sample 26 lowered 1131 m plus 223 m (2°W over 6.4 km), and sample 27 lowered 1131 m plus 362 m (2°W over 10.4 km). (c) Corrected age-elevation plot for the SG block (as in Figure 4b) along with the measured age-elevations of upper samples from the BB block (from Bear Creek Canyon, samples 15, 16, and 17). The two sets of age-elevations align more closely when the localized warp of the SG block has been removed.

the block (sample 27, San Gorgonio Peak) (Figure 4a). The one helium age that does not fit these isochrons is from sample 25, which coincidentally lies 4.5 km to the north of the east-west line of the others (Figure 1). When projected onto this line, sample 25 is too old for its present elevation (or too low for its age) relative to these helium isochrons, suggesting uplift of the SG block increases to the south.

The helium ages of the SG block thus seem to reflect a similar variation in uplift magnitude as implied by geologic data. This can be further evaluated by restoring the deformation suggested by geologic features and observing the resulting relationship between helium age and elevation. The patches of weathered granite atop the block suggest northward tilting of ~10°, which is the basis for adjusting the elevation of sample 25 relative to the other samples that fall along an approximate east-west line. Once the northward tilt is restored, the age of sample 25 fits the isochronous surfaces constructed from other ages (Figure 4a). The topography and weathered surface also suggest westward tilting of the block, but these do not offer tight constraints on the magnitude of tilting because of possible erosion and limited preservation of the surface. The helium isochrons have a convex shape that can be approximated by a ~2° down-to-the-west tilt from the center of the block (sample 27) to sample 25 and a ~5.5°

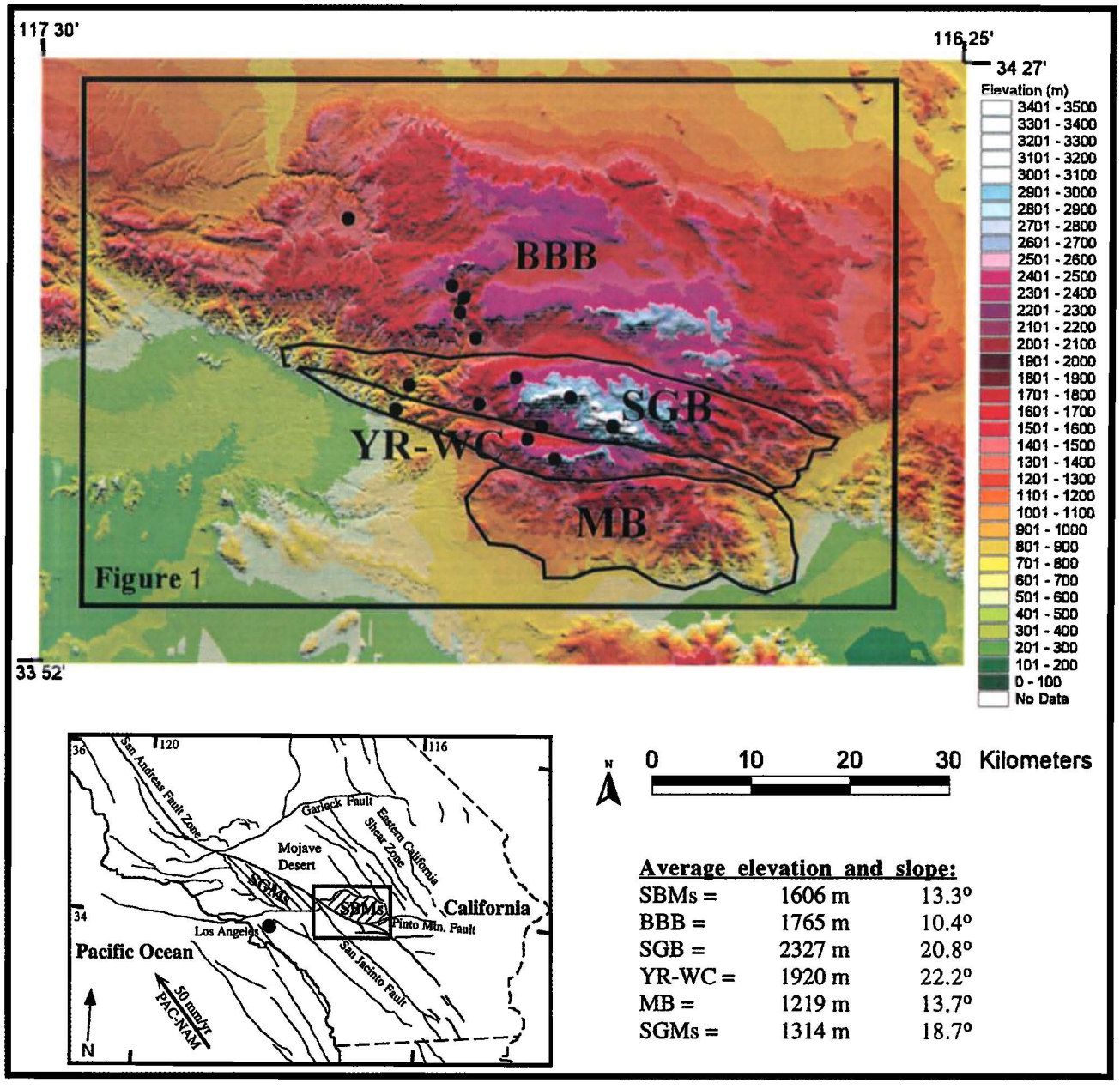

Plate 1. Digital elevation model of the San Bernardino Mountains (SBMs), color coded for elevation. Elevation divisions are 100 m, as shown by the scale on the right, and increase from dark green (low elevation) to white (high elevation). Note that the elevation model is shaded for relief (lit from the north), so that colors may be darker on the map than on the legend. Inset shows location of the SBMs and the digital elevation model (boxed) relative to the San Andreas fault zone, San Gabriel Mountains (SGMs), and velocity of the Pacific Plate relative to the North American Plate (NUVEL-1A CFR, [*DeMets*, 1995]) in southern California. Circles show the approximate locations of helium samples (refer to Figure 1 for numbers). The Big Bear block makes up the broad northern plateau, and the tectonic blocks in the southern part of the range are outlined. The average elevation and slope of the SBMs and SGMs, as well as that of the major tectonic blocks, are listed in the lower right. These parameters are based on the 90-m resolution digital elevation model, from which this map was generated. Abbreviations are as follows: BBB, Big Bear block; SGB, San Gorgonio block; YR-WC, Yucaipa Ridge-Wilson Creek blocks; and MB, Morongo block.

westward tilt from samples 25 to 20 (Figure 4a). This geometry is consistent with the geomorphic indicators and is thus used as the basis for correcting sample elevations. These westward tilts are restored by holding the elevation of sample 20 fixed and lowering samples successively greater amounts to the east.

Once this deformation has been restored, the relationship between helium age and corrected elevation in the SG block is much more uniform (Figure 4b). The resulting age-elevation gradient is about 26 Myr/km, the same as calculated from two sample pairs that are separated by substantial relief and minimal lateral distance within the block. This gradient is also comparable to that in the BB block. The elevation adjustments reduce the SG block samples to similar elevations as the BB block samples of similar age (Figure 4c) and compress the relief of the SG block to be more similar to that of the BB block. This supports the hypothesis that the two blocks expose similar structural levels that were aligned during Tertiary cooling and argues that their weathered surfaces are correlative, despite their separation by the structurally low Santa Ana Valley.

Helium ages are thus consistent with the structural hypothesis of local warping of the western SG block that is suggested by other geologic and geomorphic data. The topography of the eastern half of the block suggests a similar warp down to the east. This pattern of differential uplift is reminiscent of a gentle, north-south trending antiform that plunges moderately to the north. Because samples south of the crest of the block do not appear tilted downward to the south, the structure does not appear to have a south plunging limb. Helium ages would have to be determined from the eastern half of the block to confirm whether an eastern limb exists as well. The maximum elevation adjustment in the restoration of this deformation (~1.5 km, sample 27) is slightly greater than the difference in elevation of the crests of both blocks (~1.3 km). This suggests minor erosion has occurred atop the south central portion of the SG block, consistent with the preservation of only tiny patches of weathered granite on the northwestern part of the block (Figure 1). The westward tilt indicated by isochronous surfaces in the SG block is also less steep than the topographic surface (Figure 4a). This suggests that the relief of the block is a function of both uplift (greater in the center) and erosion (greater on the west).

5.3 Yucaipa Ridge and Wilson Creek Blocks

The very young helium ages determined on samples from the southern blocks indicate that they only recently cooled below the temperature range of helium partial retention in apatite. The ages are probably related in some way to activity of the San Andreas fault system because of their locations between its strands.

The corresponding closure temperatures and depths for these ages depend on the cooling histories and the local geothermal gradient. Owing to the proximity to the San Andreas fault, there is the possibility that fault friction produced heat that resulted in a locally high geothermal gradient, so that the young helium ages might reflect exhumation from only the shallowest crustal levels. In this case, elevated lateral heat flow from the fault would be observed in elevated vertical geothermal gradients on either side of the fault. However, the San Andreas lacks the heat flow anomaly expected if fault friction were high. Average heat flow measurements of ~70 mW/m^2 in the vicinity of the southern San Andreas fault correspond to geothermal gradients of ~30°C/km and are inconsistent with a near-fault heat anomaly [*Turcotte and Schubert*, 1982, p. 136; *Lachenbruch et al.*, 1985; *Lachenbruch and Sass*, 1988]. A slightly higher geothermal gradient was measured along the San Andreas fault to the northwest in the scientific well at Cajon Pass, but this has been explained as a transient phenomenon due to very recent erosion of overburden rather than fault friction [*Sass et al.*, 1992]. These gradients indicate that the partial retention zone of helium is several kilometers beneath the surface, and thus the young ages represent significant recent exhumation, not local heating. A possible exception to this could be that hot fluids migrated upward along fractures to heat samples at very shallow crustal levels. However, it seems unlikely that all three young samples would have been so similarly affected by such a nonuniform process, whereas old samples in the SG block that are equally close to the San Andreas fault fail to exhibit any such effect (Figure 1).

We thus propose that the young ages of the YR and WC blocks reflect cooling due to recent exhumation from significant depth. To interpret the magnitude and rate of this exhumation, it is necessary to make several assumptions. First, we assume that the present-day geothermal gradient of ~30°C/km (and ambient surface temperature of ~15°C) has been constant for the past few Myr. This assumption requires that perturbations of the thermal gradient due to uneven surface topography have been small. Given the narrow width (<5 km) of the present-day YR and WC blocks, it is likely that the gradient is not strongly disrupted by their ≤1-km relief [*Mancktelow and Grasemann*, 1997]. However, we do not know how their topography has varied in the past, nor to what degree the high San Gabriel Mountains insulated the southern SBMs as they passed alongside over the past few Myr because of displacement along the San Andreas fault zone. In addition, it is not certain to what degree isotherms were advected upward during the rapid (see below) exhumation of the YR and WC blocks [*Mancktelow and Grasemann*, 1997]. Given the lack of control on these important factors, however, we have chosen to assume the simplest case of a constant geothermal gradient, in order to infer physical meaning from these young helium ages.

On the basis of these assumptions and assuming monotonic cooling, the samples from the YR block had to have been within the depth range of helium partial retention (~1-3 km, or hotter than 40°C and colder than 100°C) at 1.6 Ma. If hotter than 100°C after 1.6 Ma, they would not have accumulated enough helium to be this old. If cooler than 40°C prior to 1.6 Ma, they would have accumulated too much helium and would be too old. Although the same is true for the 0.7 Ma sample from the

WC block, the cooling history of this block is more difficult to interpret. Suites of helium ages more tightly constrain a thermal history than does a single sample age, and the exhumation histories of the YR and WC blocks cannot be interpreted jointly because of the poor constraint on the slip history of the intervening Wilson Creek fault (Figure 1). In addition, the presence of the Mill Creek Formation (10-13 Ma) in the WC block (Figure 1) requires that both subsidence (i.e., transtension) and uplift (i.e., transpression) have occurred since the mid-Miocene [*Sadler et al.*, 1993]. For these reasons, we focus our interpretation on the magnitude and rate of exhumation of the YR block.

Given that the ages from the YR block are so young (1.6 Ma), their large errors (±0.5 Ma) significantly affect interpretations of cooling/uplift history. If the average ages are accepted at face value, their similarity suggests that the two samples shared cooling histories and exhumed from the helium partial retention zone at roughly the same time. Because these samples were separated by ~1-km elevation (Table 1), this scenario implies extremely rapid exhumation over a short period. For example, 4 km of exhumation at 10 mm/yr between 1.7 and 1.3 Ma would have resulted in nearly identical upper and lower ages (1.6 and 1.5 Ma), based on numerical solutions to the helium production/diffusion equation and the above geothermal gradient. Although even more rapid exhumation rates are permitted by these data, much slower YR block cooling is also possible given the large error bars. For example, exhumation of the block at a constant rate of 1.5 mm/yr over the past few Myr would have produced upper and lower ages of 2.1 Ma (within error limits of sample 21) and 1.6 Ma (sample 23). In another possible case, exhumation at 2.25 mm/yr could have produced an upper age of 1.6 Ma (sample 21) and a lower age of 1.1 Ma (within error limits of sample 23). Both of these cases of uniform uplift predict ~3-4 km total exhumation occurred in the past 2 Myr.

More complex thermal histories are also permitted by the data, but more helium ages would have to be determined to further constrain the exhumation history of the YR block. We hope to pursue a more rigorous collection and analysis of samples from this block to improve our understanding of its thermal history. Regardless of cooling history, however, the young ages require roughly 3-4 km of exhumation in the past 2 Myr, given the above assumptions. Because there are no older helium ages from the YR block, there is also no constraint on how much exhumation occurred prior to 2 Ma.

If the YR block has risen at least ~3-4 km in the past 2 Myr, the present topography (just over 1-km relief above base level) requires at least 2-3 km of crust to have been removed by erosion. This suggests that the top of the YR block would stand at least 1 km higher than the present crest of the SG block if no erosion had occurred over the past few Myr (Figure 5). Even more exhumation and erosion may have occurred prior to this. In addition, the minimum uplift rate required for post-2-Ma exhumation is ~1.5 mm/yr. This rate could be much higher, as shown above, and could rival those observed in other orogenic environments such as the Himalayas [*Burbank and Beck*, 1991].

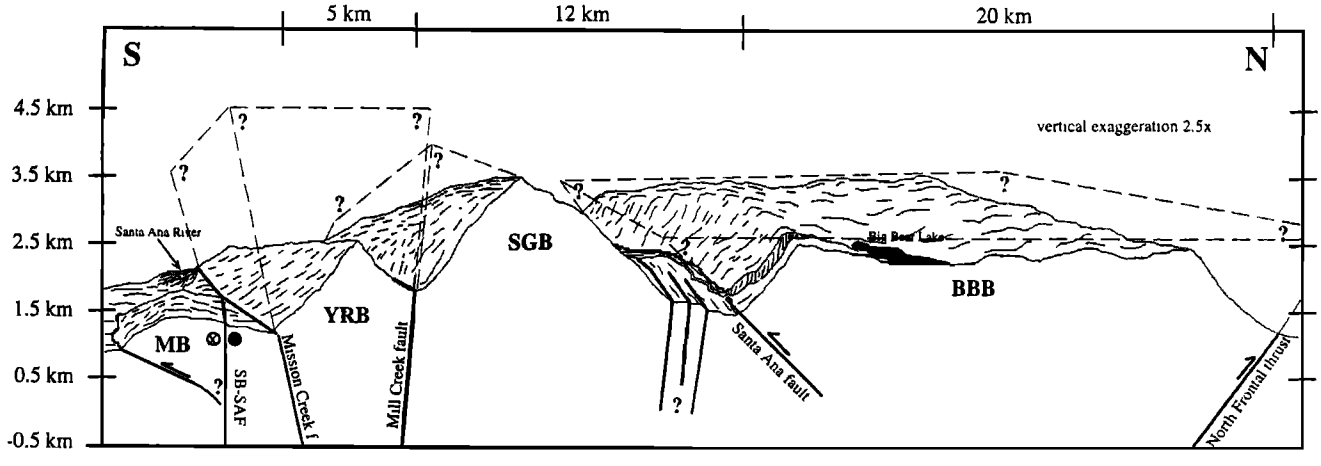

Figure 5. Schematic block diagram of the San Bernardino Mountains along a north-south transect, showing our interpretation of the relief of major blocks if no erosion had occurred in the last few Myr. The solid line shows the present-day topography along a north-south transect (line of section shown in Figure 1, vertical exaggeration is 2.5 times). The dashed lines represent the relief of the blocks when erosion is restored. Major faults are shown with approximate dips [*Allen*, 1957; *Meisling*, 1984; *Sadler*, 1993]. The Yucaipa Ridge block may have stood at an elevation of ~4.5 km, one kilometer higher than the present-day crest of the San Gorgonio block and 2 km higher than the Big Bear block. The San Gorgonio block is shown tilting upward to the south, and the Big Bear block is shown with only minor erosion restored from the top of the plateau and weathered granite surface. Abbreviations are as follows: MB, Morongo block; YRB, Yucaipa Ridge block; SGB, San Gorgonio block; BBB, Big Bear block; and SB-SAF, San Bernardino strand of the San Andreas fault zone.

6. Implications for the Role of the San Andreas Fault in Uplift

Helium ages from the SBMs provide new constraints on the timing and amount of exhumation and uplift beyond what has been determined by other geologic observations. The amount of recent uplift within each fault-bounded block is, as suggested by the greater elevation and ruggedness of topography, greater in the south than in the north (Figure 5). This greater uplift of the southern SBMs coincides with the most rapid uplift suggested by geodetic data in southern California [*Castle and Gilmore*, 1992]. Leveling data suggest that uplift over the past few decades may have proceeded at rates greater than ~1 cm/yr in the southern SBMs, which could suggest that the rapid uplift of the southern blocks is continuing. Although short-term (<100 yr) geodetic data may not reflect the long-term (> 1 Myr) uplift history of a region and the geodetic evidence of this uplift is controversial [cf. *Stein et al.*, 1986], the comparison with rates from helium ages is intriguing.

Helium ages offer uplift constraints that can be used as arguments in structural interpretation of the SBMs. Old helium ages from the BB block are consistent with the hypothesis that its central portion has risen uniformly, presumably as the hanging wall block of the North Frontal thrust system and perhaps along the Santa Ana thrust, and that its plateau has had minimal erosion and internal deformation over the last few Myr. These ages neither confirm nor refute geological observations that suggest the block began rising between 2 and 3 Ma [*Meisling and Weldon*, 1989; *May and Repenning*, 1982]. They also fail to record whether uplift has been uniform since then, although the sizes and ages of scarps along the bounding thrust faults argue that uplift rate has been decreasing throughout the Pleistocene [*Meisling and Weldon*, 1989; *Sadler*, 1993].

South of the BB block, the magnitude of vertical displacement is much more irregular. The Santa Ana Valley to the south sits 1 km below the BB block and is a structural low rather than a recent incision [*Sadler*, 1993] (Figure 1). Helium ages from farther south indicate the SG block has been uplifted by as much as 1.5 km above the BB block and even more relative to the valley. Ages from the YR and WC blocks suggest uplift on the south exceeds that of the SG block by more than 1 km. The greater irregularity and magnitude of uplift on the south is difficult to explain simply with displacement on the North Frontal thrust system (Figure 5). The thrust dips southward and may flatten to extend beneath these blocks as a decollement, but significant variations in slip or geometry along the thrust would be required to produce this pattern of uplift. A simpler explanation would thus be favored.

The greater uplift on the south also significantly exceeds that expected for local isostatic compensation of valley incision. The magnitude of uplift due to local compensation depends on the volume of eroded material in a given area and the ratio of crustal and mantle densities [*Montgomery*, 1994]. The degree of local compensation is also limited by the flexural rigidity and lateral dimension of a mountain block. On the basis of a probable range of flexural rigidities of 10^{21}-10^{23} N m (south and north plates [*Li et al.*, 1992; *Sheffels and McNutt*, 1986]), a length scale of 10^{1}-10^{2} km, a 0.8-crust/mantle density ratio, and a ratio of eroded volume per area (akin to depth of incision) of ~1 km, the magnitude of uplift due to local compensation expected for the southern SBMs is only 0-200 m [*Montgomery*, 1994]. This is consistent with the idea that block uplift was tectonic and that the faults between them control their basic topographic form more significantly than erosion. It is also consistent with the observation that many of the low regions between the blocks, such as the Santa Ana Valley, preserve preuplift sediments and thus appear to be structurally controlled and not due to recent incision.

The greater and more localized deformation experienced by the southern blocks coincides with increased structural complexity represented by high angle faults associated with the San Andreas fault zone. We thus propose that these faults are responsible for the observed vertical motions of crustal blocks and that the San Andreas fault played a significant role in uplift of the southern SBMs. Below, we examine the possible causes and implications of this deformation of the YR-WC and the SG blocks.

6.1 Uplift of the Yucaipa Ridge and Wilson Creek Blocks

The young helium ages from the YR and WC blocks document young cooling due to recent uplift that exceeds the magnitude of uplift experienced by blocks to the north. We propose that these blocks were squeezed up as pressure ridges along the subparallel strike-slip faults that bound them. This supports the contention of *Dibblee* [1982] that the greatest uplift in the SBMs has occurred along crustal slices within the San Andreas fault system. The mechanism by which these strike-slip faults produced uplift depends on the configuration of active strike-slip faulting at the time.

Below, we discuss plausible mechanisms of uplift for the YR block. Although the WC block uplift may have been produced by the same mechanism, these blocks are separated by the Wilson Creek fault, a major strand of the San Andreas fault system. Although this fault is likely to have been extinct by the time these blocks began to uplift, lateral motion during or after uplift are not precluded by existing evidence [*Matti et al.*, 1985]. We thus discuss the uplift of the YR block, for which we have two dated samples, and only acknowledge that the WC block may have been uplifted by a similar mechanism.

Greater uplift of the YR block relative to the SG block to the north seems to require vertical motion on the intervening Mill Creek fault (Figures 1 and 5). This is consistent with south-side-up scarps in Pleistocene alluvium [*Farley*, 1979] and slickensides along the fault [*Allen*, 1957] between Mill and Whitewater Creeks. Vertical motion may have also accumulated on the Mission Creek and San Bernardino fault strands that bound the block on the south (Figure 1). However, the

lack of helium ages from the Morongo block prevents us from knowing whether it has experienced a similar magnitude of rock uplift. The greater relief of the YR block relative to the Morongo block suggests uplift may have been localized to north of the Mission Creek fault. If the YR block did rise relative to the Morongo block, the sense and magnitude of motion would mimic the north-side-up separation of the base in seismicity (~15-20 km depth) below the surface trace of the Mission Creek fault [*Corbett*, 1984; *Webb and Kanamori*, 1985; *Magistrale and Sanders*, 1996]. The exhumation suggested by the helium ages thus appears consistent with the surrounding geologic relations.

Vertical motion along a strike-slip system can result from a number of different configurations of active faulting. For example, reverse slip can accommodate horizontal displacement if a strike-slip fault is nonvertical and there is convergence across the fault zone (Figure 6a). Such slip partitioning can occur on oblique-slip faults that are parallel to and decoupled from the main strand of a strike-slip system when the maximum horizontal stress is nearly perpendicular to the fault zone [*Mount and Suppe*, 1987]. Ruptures during the 1989 Loma Prieta and 1986 Palm Springs earthquakes are recent examples of this, in which substantial components of horizontal plate motion were accommodated by vertical slip [*Jones and Wesnousky*, 1992]. Depending on the dip of the fault, slip partitioning can result in large vertical displacements. For example, the ratio of horizontal to vertical slip on the 45° dipping rupture that produced the Palm Springs earthquake was

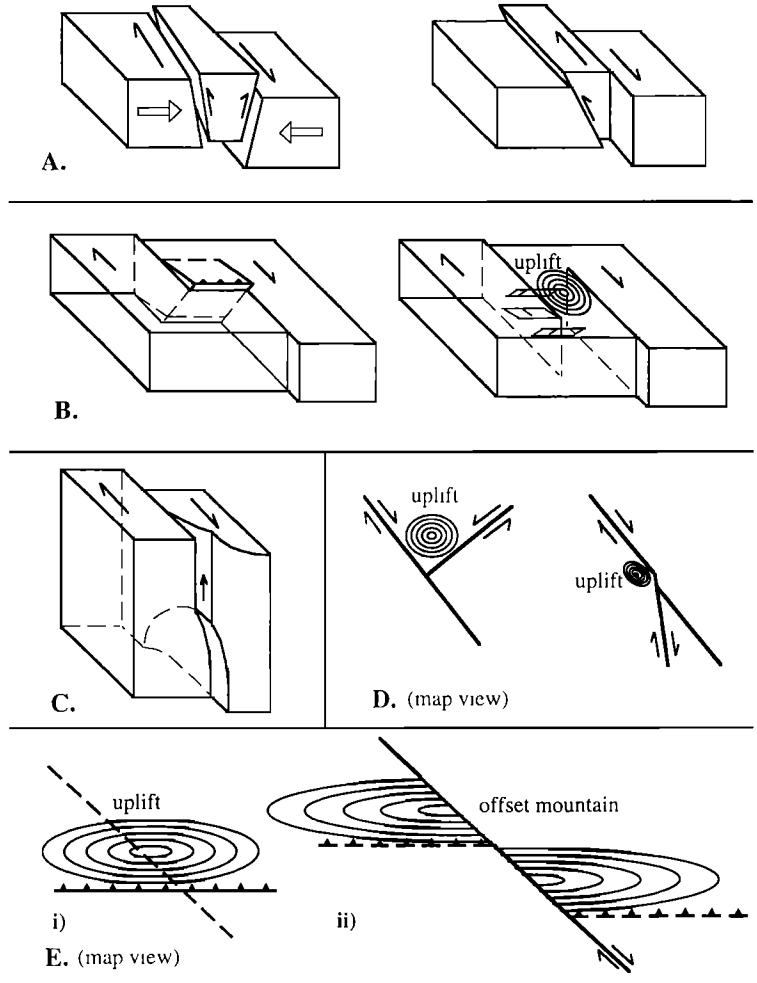

Figure 6. Generalized block diagrams that show examples of how vertical motion may occur in association with strike-slip faulting. (a) Uplift of block due to vertical motion associated with slip partitioning on a dipping fault strand in a strike-slip zone. (b) Uplift of block due to convergence within a fault stepover or restraining bend, either as a single thrust ramp or as diffuse internal shortening (concentric circles are elevation contours symbolizing uplift and small planes represent minor reverse faults at depth). (c) Uplift due to a subsurface bend or other geometric perturbation propagating along a strike-slip fault (the western San Bernardino arch [*Meisling and Weldon*, 1989]). (d) Uplift due to convergence associated with intersecting subparallel or conjugate strike-slip faults. (e) Apparent uplift along a strike-slip fault due to pure strike-slip offset of a topographic high.

nearly 3 to 1 [*Pacheco and Nabelek*, 1988]. The Mill Creek and Mission Creek faults dip moderately (~60°) southward and northward, respectively, under the YR block in present exposures (Figure 5) [*Allen*, 1957]. If these faults were active and had such dips at around 1.6 Ma, their geometry could have led to slip partitioning and the exhumation of the YR block. For example, a 60° dip on the Mill Creek fault, a 30° angle between it and the regional direction of strike-slip motion, and ~3-4 km of YR block rock uplift translate to about 3.5-4.6 km of dextral slip accommodated by vertical motion on the Mill Creek fault in the last 1.6 Myr (about 10% of the total San Andreas slip in 1.6 Myr [*Weldon and Sieh*, 1985]). More strike-slip motion may have been accommodated by uplift prior to this.

A second configuration of active strike-slip faulting that can result in vertical motion is that of a contractional fault stepover or restraining bend (Figure 6b). The YR block is situated just northwest of the 15-km-wide stepover between the San Bernardino and Coachella Valley strands of the San Andreas fault zone in San Gorgonio Pass (Figure 1). Given that a minimum of 8-10 km of right slip has taken place across the Mill Creek fault in the Pleistocene [*Matti et al.*, 1985], the YR block could have been located in this stepover region during its exhumation. Convergence in this stepover could have produced uplift by north-south thrusting on a major ramp structure, such as the modern San Gorgonio Pass fault zone [*Allen*, 1957; *Matti et al.*, 1985], or more diffuse internal deformation [*Nicholson et al.*, 1986] (Figure 6b). Such north-south convergence is evident in recent seismicity in the present-day San Gorgonio Pass block [*Seeber and Armbruster*, 1995]. The restoration of the volume (i.e., mass balance) of the uplifted YR block (minimum of ~3 km exhumed times ~15 km length times ~4.5 km width equals ~200 km^3) back into the 15-km-wide by 15-km-deep stepover requires ~1 km of fault-parallel convergence. This is only about 5% of the total convergence that would have occurred in 1.6 Myr if all of the San Andreas fault motion was accommodated (25 mm/yr times 1.6 Ma equals 40 km [*Weldon and Sieh*, 1985]). Hence the uplift of the block could easily have resulted from this mechanism. The present-day Morongo block may be a nascent expression of this mechanism (Figure 5).

These two possible explanations seem equally likely, and although we cannot determine which plays a greater role, both are favored over other possible explanations. In order to test these hypotheses, exact knowledge of the relative position of the block through the past few Myr due to strike-slip faulting would be needed. Several other possible causes of the recent uplift of the YR block include the following. One possibility is that the YR block was deformed by a subsurface bulge propagating along one of the strands of the San Andreas fault (Figure 6c). This has been proposed to explain local tilting of sediments that has migrated to the northwest at approximately the rate of slip on the San Andreas fault in the northwesternmost SBMs (the western San Bernardino arch [*Meisling and Weldon*, 1989]). However, this specific subsurface geometric perturbation was beneath Lake Arrowhead (25 km northwest of the YR block) at ~1.5 Ma [*Meisling and Weldon*, 1989], making it an unlikely cause for YR block uplift. A similar subsurface geometric perturbation could have existed to the south during the time of YR block uplift. A second possibility is that local convergence and uplift along the San Andreas fault has resulted from its intersection with other strike-slip faults, such as the Pinto Mountain or San Jacinto faults (Figures 1 and 6d) [*Dibblee*, 1975]. This could be similar to the convergence that produced uplift at the intersection of the San Andreas and Garlock faults to the northwest [*Bohannon and Howell*, 1982].

A final possibility is that the uplift was produced by a structure that has subsequently been offset laterally along the San Andreas fault. The young helium ages from the YR block could be related to young fission track ages determined for rocks of the San Gabriel Mountains to the west [*Blythe et al.*, 1996], if the Cucamonga thrust system had uplifted them together prior to large lateral displacement (Figure 6e). In this case, the Banning fault (or San Gorgonio Pass fault zone) could be a stranded section of the Cucamonga thrust and may have uplifted the entire region between it and the Mill Creek strand. Determining helium ages within the Morongo block to the south of the YR block would help to test this hypothesis. The proposal seems unlikely, however, because of the timing of uplift and strike slip. Given the present slip rates on the San Andreas and San Jacinto faults [*Weldon and Sieh*, 1985], the 50-km separation between the San Gabriel Mountains and YR block would have accrued in ~1.5 Myr or more (depending on what fraction of the slip occurred on the Mill Creek fault, Figure 1). The San Gabriel Mountains may have been uplifting continuously since then, however, based on the similarity between modern (faulted alluvium) and long-term (fission track on bedrock) rates of uplift [*Dolan et al.*, 1996; A. Blythe, personal communication, 1997]. In addition, helium ages argue that significant exhumation had to proceed the time when the San Gabriel Mountains were adjacent to the YR and WC blocks, when samples were likely still within the helium partial retention zone (several kilometers deep). The hypothesis thus seems unlikely, although it cannot presently be ruled out.

6.2 Deformation of the San Gorgonio Block

Like the YR block, the helium ages from the SG block imply that it has been deformed and uplifted more than the BB block (Figure 5). The deformation that produced this structure may have been localized by the faults that bound it, such as the Mill Creek strand of the San Andreas fault zone on the south and the unnamed high-angle, oblique (south-side-up and dextral) structures that break sediments and juxtapose sediments and SG block basement to the north in Santa Ana Valley [*Dibblee*, 1964; *Jacobs*, 1982; *Sadler*, 1993] (Figure 1). Displacement on the northern faults is required, given that the down to the north tilting is not sufficient to explain the total relief between the weathered granite surfaces atop the SG block and the structural low of Santa Ana Valley (Figure 3). It is thus likely that the local warping of the SG block resulted from

a geometric complexity along a strike-slip fault system, similar to mechanisms illustrated in Figure 6.

Unlike the YR block, the helium ages from the SG block do not constrain when this local deformation occurred. The youngest feature that shows the northward block tilting is the Mio-Pliocene Santa Ana sandstone. This unit contains clasts from the San Gabriel Mountains that would have been transported northward prior to uplift of the SG block and thus constrains uplift of the block to after 4 Ma (unless substantial lateral offset has occurred along the structures between the SG block and Santa Ana Valley [*Sadler*, 1993]). There is no upper constraint to the timing of uplift of the SG block, however, and it could be rising today. Without knowing when this deformation occurred, we can only speculate on what produced it.

The geometry of SG block deformation offers some hints as to how it was produced. The apparent northward and westward tilt of isochronous surfaces and geologic features, as well as the east and west slope of the SG ridge line, suggest that the block is an elongate, northward plunging, north-south trending antiform. The shape of the antiform indicates east-west shortening and localized uplift on the south, with the maximum amplitude centered at San Gorgonio Peak (sample 27, Figure 1). Because the folding postdates helium ages (i.e., cooler than 40°C), it is unlikely that it could have been due to ductile deformation of crystalline rock. It is also unlikely that the fold was created by pure elastic bending, given that the magnitude of uplift varies 1.5 km over ~22 km distance (~7% strain) (Figures 1 and 4). The warping of the block may thus have been produced by internal brittle deformation. Folding could have been produced by displacement on the Mill Creek fault if it had a significant component of reverse slip along the center of the SG block that gradually gave way to pure strike slip in either direction (Figure 1). Such a reverse component of slip could have resulted from convergence in San Gorgonio Pass or simply the orientation of the fault relative to the regional direction of right shear. The convergence accommodated by the SG block uplift is of the same order as that accommodated by the YR block (~1 km), based on the volume restoration of the SG block's greater lateral extent and smaller magnitude of uplift (Figures 1 and 5).

7. Conclusions

Radiogenic helium thermochronometry offers new constraints on the tectonic development of the San Bernardino Mountains. Paleocene to Miocene helium ages from the Big Bear block show that very little exhumation has taken place there since the Late Cretaceous. The geometry of the isochronous surfaces are consistent with the hypotheses that the block's surface has been only slightly eroded since exposed to deep weathering in the late Miocene and that the block was uplifted as an intact massif, presumably as the hanging wall block the North Frontal thrust system and Santa Ana thrust.

Helium ages from the San Gorgonio block are similar to those from the Big Bear block (~56-14 Ma) and predate the recent uplift of the San Bernardino Mountains. The geometry of isochronous surfaces constructed from these ages suggests that the weathered granitic surface atop the block was originally continuous with that atop the Big Bear plateau. This implies that the San Gorgonio block has experienced roughly 1.5 km more uplift than the Big Bear block and that this uplift is mimicked by the topographic form of the block. The structure of the block appears to be a gentle antiform, based on the orientations of geologic datums and warped isochronous surfaces. Such a structure is better explained by uplift due to local complexities associated with the high-angle faults that bound it than slip along the North Frontal thrust system that has produced more uniform uplift of the Big Bear plateau. We speculate that convergence associated with geometric complexities along the San Andreas fault zone produced this structure, but lack of constraint on the exact timing of this deformation prevents knowing what configuration of faulting was active at the time.

The helium ages from the Wilson Creek and Yucaipa Ridge blocks within the San Andreas fault zone are very young (0.7-1.6 Ma) and indicate recent, rapid cooling. These ages suggest thermal histories that require ≥3-4 km of uplift in the past few Myr. This magnitude of uplift indicates that the Yucaipa Ridge block would have stood at least 1 km above the present topography of the San Gorgonio block, if no erosion had occurred. Such uplift would have proceeded at a rate of ≥1.5 mm/yr but may have been shorter lived at a rate ≥10 mm/yr. This high rate and magnitude of uplift is confined to crustal slices within the San Andreas fault zone and implies local uplift associated with strike-slip faulting as opposed to displacement on the North Frontal thrust system. The uplift rate may have been a significant component of the total slip rate across the strike-slip system. As in the case of the San Gorgonio block, this uplift may have resulted from geometrical complexities along the San Andreas fault.

These results imply that the San Bernardino Mountains consist of several tectonic blocks that have risen because of both thrusting and oblique slip associated with complexities along the San Andreas fault zone on the south. Transpression thus appears to have occurred in several modes, which include significant magnitudes of vertical motion along the San Andreas fault itself. Likewise, a significant component of San Andreas fault motion was probably accommodated by uplift that resulted from convergence.

Acknowledgments. We thank Martha House and Rich Wolf for significant help with lab work, Doug Yule for help with sample collection, and Martha, Rich, Doug, Andrew Meigs, and Lee Silver for valuable help with interpretations and regional geology. We also thank Robert Castle and Peter Sadler for helpful reviews of this manuscript. This project was funded by the National Science Foundation and U.S. Geological Survey through the Southern California Earthquake Center (contribution 379). This is Seismological Laboratory of California Institute of Technology contribution 6205.

References

Allen, C.R., San Andreas fault zone in San Gorgonio Pass, southern California, *Geol. Soc. Am. Bull., 68*, 315-350, 1957.

Blythe, A.E., E.J. Fielding, and D.W. Burbank, Morphology as a function of bedrock uplift and climate: A case study of the Transverse Ranges, southern California, from apatite fission track and DEM analysis (abstract), *EOS Trans., AGU, 77* (46), Fall Meet. Suppl., F644, 1996.

Bohannon, R.G., and D.G. Howell, Kinematic evolution of the junction of the San Andreas, Garlock, and Big Pine faults, California, *Geology, 10*, 358-363, 1982.

Bortugno, E.J., and T.E. Spittler, Geologic map of the San Bernardino Quadrangle, California, 1:250,000 scale, *Reg. Geologic Map Ser., Map 3A*, Calif. Div. Mines Geol., 1986.

Burbank, D.W., and R.A. Beck, Rapid, long-term rates of denudation, *Geology, 19*, 1169-1172, 1991.

Castle, R.O., and T.D. Gilmore, A revised configuration of the southern California uplift, *Geol. Soc. Am. Bull., 104*, 1577-1591, 1992.

Corbett, E.J., Seismicity and crustal structure of southern California: Tectonic implications from improved earthquake locations, Ph.D. thesis, 231 pp., Calif. Inst. of Technol., Pasadena, Calif., 1984.

DeMets, C., Reappraisal of seafloor spreading lineations in the Gulf of California: Implications for the transfer of Baja California to the Pacific Plate and estimates of Pacific-North America motion, *Geophys. Res. Lett., 22*, 3545-3548, 1995.

Dibblee, T.W., Geologic map of the San Gorgonio Mountain 15' Quadrangle, 1:62,500 scale, *U.S. Geol. Surv. Misc. Geologic Invest. Map, I-431*, 1964.

Dibblee, T.W., Geologic map of the Redlands 15' Quadrangle, 1:62,500 scale, *U.S. Geol. Surv. Open File Map, 74-1022*, 1968.

Dibblee, T.W., Late Quaternary uplift of the San Bernardino Mountains on the San Andreas and related faults, in *San Andreas Fault in Southern California*, edited by J.C. Crowell, *Spec. Rep. Calif. Div. Mines Geol., 118*, 127-135, 1975.

Dibblee, T.W., Geology of the San Bernardino Mountains, southern California, in *Geology and Mineral Wealth of the California Transverse Ranges*, edited by D.L. Fife and J.A. Minch, pp.148-169, South Coast Geol. Soc., Santa Ana, Calif., 1982.

Dodson, M.H., Closure temperature in cooling geochronological and petrological systems, *Contrib. Mineral. Petrol., 40*, 259-274, 1973.

Dolan, J.F., F. Jordon, G. Rasmussen, D. Stevens, W. Reeder, and L.M. McFadden, Evidence for probable moderate-sized (*Mw* 6.5-7.0) paleoearthquake on the Cucamonga Fault, northwestern Los Angeles metropolitan region, California (abstract), *EOS Trans., AGU, 77* (46), Fall Meet. Suppl., F461, 1996.

England, P., and P. Molnar, Surface uplift, uplift of rocks, and exhumation of rocks, *Geology, 18*, 1173-1177, 1990.

Farley, K.A., R.A. Wolf, and L.T. Silver, The effects of long alpha-stopping distances on (U-Th)/He dates, *Geochim. Cosmochim. Acta, 60*, 4223-4229, 1996.

Farley, T., Geology of a part of northern San Gorgonio Pass, California, M.S. thesis, 159 pp., Calif. State Univ., Los Angeles, 1979.

Foster, D.A., D.S. Miller, and C.F. Miller, Tertiary extension in the Old Woman Mountains area, California: Evidence from apatite fission track analysis, *Tectonics, 10*, 875-886, 1991.

Frizzel, V.A., J.M. Mattinson, and J.C. Matti, Distinctive Triassic megaporphyritic monzogranite: Evidence for only 160 km offset along the San Andreas fault, southern California, *J. Geophys. Res., 91*, 14080-14088, 1986.

George, R.G., and R.K. Dokka, Major Late Cretaceous cooling events in the eastern Peninsular Ranges, California, and their implications for Cordilleran tectonics, *Geol. Soc. Am. Bull., 106*, 903-914, 1994.

Gleadow, A.J.W., and P.G. Fitzgerald, Uplift history and structure of the Transantarctic Mountains - New evidence from fission-track dating of basement apatites in the Dry Valley area, southern Victoria Land, *Earth Planet. Sci. Lett., 82*, 1-14, 1987.

House, M.A., B.P. Wernicke, K.A. Farley, and T.A. Dumitru, Cenozoic thermal evolution of the central Sierra Nevada from (U-Th)/He thermochronometry, *Earth Planet. Sci. Lett., 151*, 167-179, 1997.

Jacobs, S.E., Geology of a part of the upper Santa Ana River Valley, San Bernardino Mountains, San Bernardino County, California, M.S. thesis, 107 pp., Calif. State Univ., Los Angeles, 1982.

Jones, C.H., and S.G. Wesnousky, Variations in strength and slip rate along the San Andreas fault system, *Science, 256*, 83-86, 1992.

Jones, L.M., E. Hauksson, and H. Qian, Where is the San Andreas Fault in the San Bernardino Mountains of southern California ?, *Seismol. Res. Lett., 64*, 22, 1993.

Lachenbruch, A.H., and J.H. Sass, The stress heat-flow paradox and thermal results from Cajon Pass, *Geophys. Res. Lett., 15*, 981-984, 1988.

Lachenbruch, A.H., J.H. Sass, and S.P. Galanis Jr., Heat flow in southern California and the origin of the Salton Trough, *J. Geophys. Res., 90*, 6709-6736, 1985.

Li, Y.-G., T.L. Henyey, and P.C. Leary, Seismic reflection constraints on the structure of the crust beneath the San Bernardino Mountains, Transverse Ranges, southern California, *J. Geophys. Res., 97*, 8817-8830, 1992.

Lippolt, H.J., M. Leitz, R.S. Wernicke, and B. Hagedorn, (Uranium + thorium) / helium dating of apatite: Experience with samples from different geochemical environments, *Chem. Geol. Isot. Geosci., 112*, 179-191, 1994.

Magistrale, H., and C. Sanders, Evidence from precise earthquake hypocenters for segmentation of the San Andreas fault in San Gorgonio Pass, *J. Geophys. Res., 101*, 3031-3044. 1996.

Mancktelow, N.S. and B. Grasemann, Time dependent effects of heat advection and topography on cooling histories during erosion, *Tectonophysics, 270*, 167-195, 1997.

Masek, J.G., B.L. Isacks, T.L. Gubbels, and E.J. Fielding, Erosion and tectonics at the margins of continental plateaus, *J. Geophys. Res., 99*, 13941-13956, 1994.

Matti, J.C., and D.M. Morton, Paleogeographic evolution of the San Andreas fault in southern California: A reconstruction based on a new cross-fault correlation, in *The San Andreas Fault System: Displacement, Palinspastic Reconstruction and Geologic Evolution*, edited by R.E. Powell, R.J. Weldon, and J.C. Matti, *Mem. Geol. Soc. Am., 178*, 107-160, 1993.

Matti, J.C., D.M. Morton, and B.F. Cox, Distribution and geologic relations of fault systems in the vicinity of the central Transverse Ranges, southern California, *U.S. Geol. Surv. Open File Rep., 85-365*, 27 pp., 1985.

May, S.R., and Repenning, C.A., New evidence for the age of the Old Woman sandstone, Mojave Desert, California, in *Late Cenozoic Stratigraphy and Structure of the San Bernardino Mountains, Field Trip 6*, edited by P.M. Sadler and M.A. Kooser, in *Geologic Excursions in the Transverse Ranges, Geol. Soc. Am. Cordilleran Sect. Meet. Guideb., 78*, edited by J.D. Cooper, pp. 93-96, 1982.

Meisling, K.E., Neotectonics of the north frontal fault system of the San Bernardino Mountains: Cajon Pass to Lucerne Valley, California, Ph.D. thesis, 394 pp., Calif. Inst. of Technol., Pasadena, Calif., 1984.

Meisling, K.E., and R.J. Weldon, Late Cenozoic tectonics of the northwestern San Bernardino Mountains, southern CA, *Geol. Soc. Am. Bull., 101*, 106-128, 1989.

Miller, F.K., and D.M. Morton, Potassium-argon geochronology of the eastern Transverse Ranges and southern Mojave Desert, southern California, *U.S. Geol. Surv. Prof. Pap., 1152*, 30 pp., 1980.

Molnar, P., and P. England, Late Cenozoic uplift of mountain ranges and global climate change: Chicken or egg ?, *Nature, 346*, 29-34, 1990.

Montgomery, D.R., Valley incision and the uplift of mountain peaks, *J. Geophys. Res., 99*, 13913-13921, 1994.

Mount, V.S., and J. Suppe, State of stress near the San Andreas fault: Implications for wrench tectonics, *Geology, 15*, 1143-1146, 1987.

Neville, S.L., and J.M. Chambers, Late Miocene alkaline volcanism, northeastern San Bernardino Mountains and adjacent Mojave Desert, in *Late Cenozoic*

Stratigraphy and Structure of the San Bernardino Mountains, Field Trip 6, edited by P.M. Sadler and M.A. Kooser, in *Geologic Excursions in the Transverse Ranges, Geol. Soc. Am. Cordilleran Sect. Meet. Guideb., 78*, edited by J.D. Cooper, pp. 103-106, 1982.

Nicholson, C., L. Seeber, P. Williams, and L.R. Sykes, Seismicity and fault kinematics through the eastern Transverse Ranges, California: Block rotation, strike-slip faulting, and low-angle thrusts, *J. Geophys. Res., 91*, 4891-4908, 1986.

Oberlander, T.M., Morphogenesis of granitic boulder slopes in the Mojave Desert, California, *J. Geol., 80*, 1-20, 1972.

Pacheco, J., and J. Nabelek, Source mechanisms of three moderate California earthquakes of July, 1986, *Bull. Seismol. Soc. Am., 78*, 1907-1929, 1988.

Proctor, R.J., Geology of the upper Coachella Valley area, California, *Spec. Rep. Calif. Div. Mines Geol., 94*, 8-43, 1968.

Reynolds, R.E., and W.A. Reeder, Age and fossil assemblages of the San Timoteo Formation, Riverside County, California, in *Geology Around the Margins of the Eastern San Bernardino Mountains, Pub. Inland Geol. Soc., 1*, edited by M.A. Kooser and R.E. Reynolds, pp. 51-56, Inland Geol. Soc., Redlands, Calif., 1986.

Sadler, P.M., An introduction to the San Bernardino Mountains as the product of young orogenesis, in *Late Cenozoic Stratigraphy and Structure of the San Bernardino Mountains, Field Trip 6*, edited by P.M. Sadler and M.A. Kooser, in *Geologic Excursions in the Transverse Ranges, Geol. Soc. Am. Cordilleran Sect. Meet. Guideb., 78*, edited by J.D. Cooper, pp. 57-65, 1982a.

Sadler, P.M., Provenance and structure of late Cenozoic sediments in the northeast San Bernardino Mountains, in *Late Cenozoic Stratigraphy and Structure of the San Bernardino Mountains, Field Trip 6*, edited by P.M. Sadler and M.A. Kooser, in *Geologic Excursions in the Transverse Ranges, Geol. Soc. Am. Cordilleran Sect. Meet. Guideb., 78*, edited by J.D. Cooper, pp. 83-91, 1982b.

Sadler, P.M., The Santa Ana basin of the central San Bernardino Mountains: Evidence of the timing and uplift and strike-slip relative to the San Gabriel Mountains, in *The San Andreas Fault System: Displacement, Palinspastic Reconstruction, and Geologic Evolution*, edited by R.E. Powell, R.J. Weldon, and J.C. Matti, *Mem. Geol. Soc. Am., 178*, 307-322, 1993.

Sadler, P.M., and Reeder, W.A., Upper Cenozoic, quartzite-bearing gravels of the San Bernardino Mountains, southern California; recycling and mixing as a result of transpressional uplift, in *Tectonics and Sedimentation Along Faults of the San Andreas System*, edited by D.W. Anderson and M.J. Rymer, pp. 45-57, Pacific Section, SEPM, Los Angeles, Calif., 1983.

Sadler, P.M., A. Demirer, D. West, and J.M. Hillenbrand, The Mill Creek basin, the Potato sandstone, and fault strands in the San Andreas fault south of the San Bernardino Mountains, in *The San Andreas Fault System: Displacement, Palinspastic Reconstruction, and Geologic Evolution*, edited by R.E. Powell, R.J. Weldon, and J.C. Matti, *Mem. Geol. Soc. Am., 178*, 289-306, 1993.

Sass, J.H., A.H. Lachenbruch, and T.H. Moses Jr., Heat flow from a scientific research well at Cajon Pass, California, *J. Geophys. Res., 97*, 5017-5030, 1992.

Seeber, L., and J.G. Armbruster, The San Andreas fault system through the Transverse Ranges as illuminated by earthquakes, *J. Geophys. Res., 100*, 8285-8310, 1995.

Sheffels, B., and M. McNutt, Role of subsurface loads and regional compensation in the isostatic balance of the Transverse Ranges, California: Evidence for intracontinental subduction, *J. Geophys. Res., 91*, 6419-6431, 1986.

Stein, R.S., C.T. Whalen, S.R. Holdahl, W.E. Strange, and W.R. Thatcher, Saugus-Palmdale, California, field test for refraction error in historical leveling surveys, *J. Geophys. Res.*, 91, 9031-9044, 1986.

Turcotte, D.L., and G. Schubert, *Geodynamics: Applications of Continuum Physics to Geological Problems*, 450 pp., John Wiley, New York, 1982.

Webb, T.H., and H. Kanamori, Earthquake focal mechanisms in the eastern Transverse Ranges and San Emigdio Mountains, southern California, and evidence for a regional decollement, *Bull. Seismol. Soc. Am., 75*, 735-757, 1985.

Weldon, R.J., The late Cenozoic geology of Cajon Pass: Implications for tectonics and sedimentation along the San Andreas fault, Ph.D. thesis, 400 pp., Calif. Inst. of Technol., Pasadena, Calif., 1986.

Weldon, R.J., and K. Sieh, Holocene rate of slip and tentative recurrence interval for large earthquakes on the San Andreas fault in Cajon Pass, southern California, *Geol. Soc. Am. Bull., 96*, 793-812, 1985.

Weldon, R.J., K.E. Meisling, and J. Alexander, A speculative history of the San Andreas fault in the central Transverse Ranges, California, in *The San Andreas Fault System: Displacement, Palinspastic Reconstruction, and Geologic Evolution*, edited by R.E. Powell, R.J. Weldon, and J.C. Matti, *Mem. Geol. Soc. Am., 178*, 161-198, 1993.

Wolf, R.A., The development of the (U-Th)/He thermochronometer, Ph.D. thesis, 211 pp., Calif. Inst. of Technol., Pasadena, Calif., 1997.

Wolf, R.A., K.A. Farley, and L.T. Silver, Helium diffusion and low temperature thermochronometry of apatite, *Geochim. Cosmochim. Acta, 60*, 4231-4240, 1996a.

Wolf, R.A., D. Kass, and K. Farley, Sensitivity of apatite (U-Th)/He ages to thermal history (abstract), *EOS Trans., AGU, 77* (46), Fall Meet. Suppl., F644, 1996b.

Wolf, R.A., K.A. Farley, and L.T. Silver, Assessment of (U-Th)/He thermochronometry: The low-temperature history of the San Jacinto mountains, California, *Geology, 25*, 65-68, 1997.

Woodburne, M.O., Cenozoic stratigraphy of the Transverse Ranges and adjacent areas, southern California, *Spec. Pap. Geol. Soc. Am., 162*, 91 pp., 1975.

Zeitler, P.K., A.L. Herczeg, I. McDougall, and M. Honda, U-Th-He dating of apatite: A potential thermochronometer, *Geochim. Cosmochim. Acta, 51*, 2865-2868, 1987.

K.A. Farley, K. Sieh, and J.A. Spotila, Division of Geological and Planetary Sciences, 100-23, California Institute of Technology, Pasadena, CA 91125. (e-mail: farley@gps.caltech.edu; sieh@gps.caltech.edu; spot@gps.caltech.edu)

(Received July 22, 1997;
revised January 29, 1998;
accepted February 2, 1998.)